JACS
JOURNAL OF THE AMERICAN CHEMICAL SOCIETY

Article

pubs.acs.org/JACS

Activated Singlet Exciton Fission in a Semiconducting Polymer

Andrew J. Musser,*[,†] Mohammed Al-Hashimi,[‡,∥] Margherita Maiuri,[§] Daniele Brida,[§] Martin Heeney,[‡] Giulio Cerullo,[§] Richard H. Friend,[†] and Jenny Clark[†]

[†]Cavendish Laboratory, University of Cambridge, Cambridge CB3 0HE, United Kingdom

[‡]Department of Chemistry, Imperial College London, London SW7 2AZ, United Kingdom

[§]IFN-CNR, Dipartimento di Fisica, Politecnico di Milano, I-20133 Milano, Italy

[∥]Department of Chemistry & Earth Sciences, College of Arts & Sciences, Qatar University, P.O. 2713, Doha, Qatar

Supporting Information

ABSTRACT: Singlet exciton fission is a spin-allowed process to generate two triplet excitons from a single absorbed photon. This phenomenon offers great potential in organic photovoltaics, but the mechanism remains poorly understood. Most reports to date have addressed intermolecular fission within small-molecular crystals. However, through appropriate chemical design chromophores capable of intramolecular fission can also be produced. Here we directly observe sub-100 fs activated singlet fission in a semiconducting poly(thienylenevinylene). We demonstrate that fission proceeds directly from the initial $1B_u$ exciton, contrary to current models that involve the lower-lying $2A_g$ exciton. In solution, the generated triplet pairs rapidly recombine and decay through the $2A_g$ state. In films, exciton diffusion breaks this symmetry and we observe long-lived triplets which form charge-transfer states in photovoltaic blends.

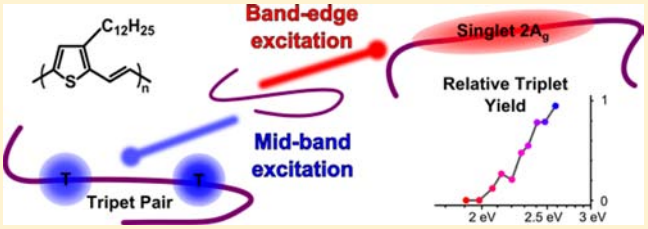

INTRODUCTION

Singlet exciton fission is a spin-allowed process in organic semiconductors whereby a singlet exciton separates into two spatially distinct spin triplet excitons.[1] First described in the 1960s, singlet fission has seen a revival of interest since the proposal that it be harnessed for carrier multiplication in organic photovoltaic devices, using one photon to generate two triplet excitons and eventually two electrons.[2] This would afford a means to overcome the Shockley-Queisser limit and increase the maximum theoretical photovoltaic power conversion efficiency from 33.7% to 44%. Singlet fission has already been implemented in solar cells,[3−7] proving the validity of the concept though efficiencies remain low. Further practical advances demand a better understanding of the mechanism(s) of singlet fission and structure−property relationships, to broaden the currently narrow library of candidate chromophores.

Most studies have focused on crystalline singlet fission sensitizers such as the acenes[8−12] and similar planar conjugated molecules.[13−15] Fission in these materials can be extremely fast (sub-100 fs) and efficient, with triplet yields often approaching 200%. The rate and yield tend to vary with intermolecular geometry and coupling, as fission is an inherently intermolecular process in such materials. A different approach that has received far less attention is to generate extended chromophores capable of undergoing intramolecular singlet fission. One means to circumvent this strong dependence on intermolecular geometry is through the use of polymers. The interactions between conjugated segments along the chain can be dominant over interchain effects,[16] and in many cases the individual chromophores should be large enough to accommodate two triplet excitons. Indeed a small set of related polymers has been shown to undergo singlet fission,[17−20] and in all cases the fission occurred within well-isolated chains. Singlet fission should thus be an inherent property of the long conjugated backbone rather than a result of intermolecular coupling. All reported examples are polyene-type structures with the lowest (dark) excited state of the same A_g symmetry as the ground state, which is theoretically predicted to be a requirement for intramolecular singlet fission.[1,21] Nonetheless, the exact mechanism of triplet generation in these materials, as well as how it relates to better-studied intermolecular fission, remains unclear.

In this work, we evaluate the role of the low-lying A_g state and study the mechanism of singlet fission in a different conjugated polymer, poly(3-dodecylthienylenevinylene) (P3TV, Figure 1). This polymer fits into the polyene class, with the important added advantages of solution-processability and stability.[22,23] Several groups have recently studied P3TV without noting the presence of singlet fission.[24−26] Their results instead reflect the conventional model of Figure 1b, in which photoexcited states decay rapidly and nonradiatively via the $2A_g$ state. Our study takes these investigations further to demonstrate conclusively the presence in P3TV of activated (i.e., occurring only above a threshold pump photon energy)

Received: May 30, 2013
Published: July 24, 2013

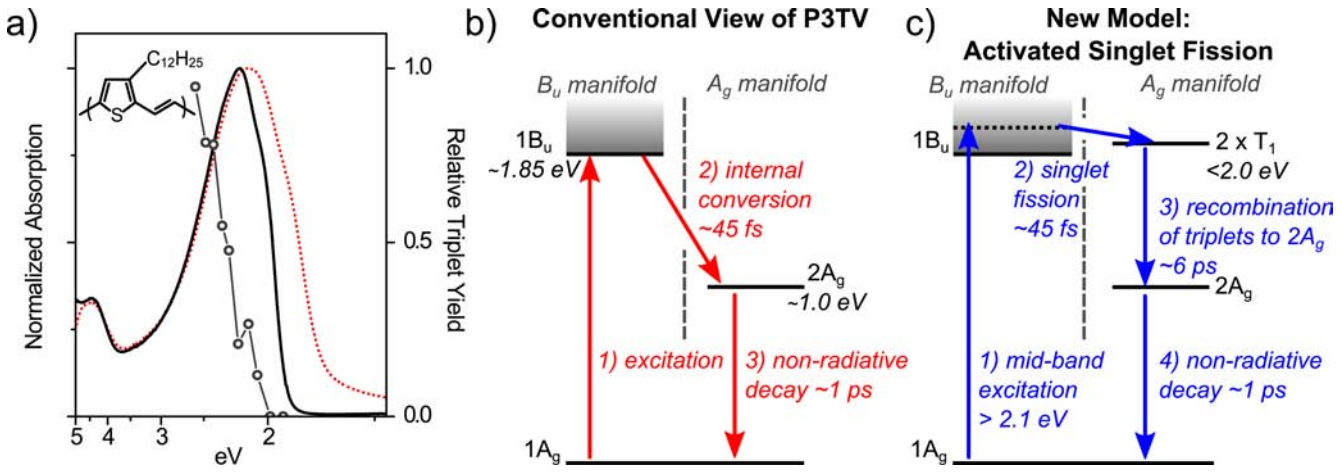

Figure 1. (a) Chemical structure of P3TV, solution (solid) and film (dotted) UV−vis absorption. Circles show the relative triplet yield obtained in solution for each pump photon energy. (b) Conventional scheme of photoexcitation in P3TV. $1B_u$ energy and time constants are as measured in this work. $2A_g$ energy is taken from ref 25. (c) For excitation energies above 2.1 eV, the new decay pathway of activated singlet fission opens. This occurs in parallel with the conventional route in (b). The limit for $2 \times T_1$ energy is determined from sensitization, as outlined in the text below.

intrachain singlet fission, depicted in Figure 1c, as a parallel decay pathway upon midband excitation. The data reveals singlet fission in solution and films and suggests it can be harnessed to generate charges in photovoltaic blends. Furthermore, since we directly observe intrachain singlet fission, we are able to show that it proceeds from the initial $1B_u$ state without passing through the $2A_g$ state. This is unexpected within the standard theoretical framework but has recently been suggested as a pathway in carotenoid aggregates[27,28] and highlights the need for further theoretical study of singlet fission in A_g-type materials.

■ EXPERIMENTAL SECTION

P3TV was synthesized as reported previously[29] with slight modifications. To 2,5-dibromo-3-dodecyl thiophene (0.25 g, 0.61 mmol) in a 2 mL microwave vial was added $Pd(PPh_3)_4$ (1 mol %, 7 mg), chlorobenzene (0.6 mL), and (*E*)-1,2, bis (tributylstannyl)-ethylene (370 mg, 0.61 mmol). The resultant mixture was degassed for 30 min with argon and securely sealed. The glass vial was heated in a microwave reactor (Biotage Initiator, constant heating mode) at 120 °C for 5 min, 140 °C for 5 min, and then 180 °C for 30 min. After being cooled to 50 °C, the reaction mixture was precipitated into a mixture of methanol (200 mL) and concentrated hydrochloric acid (2 mL). The precipitate was filtered and extracted (Soxhlet) with methanol and acetone. The remaining polymer was dissolved in chloroform and precipitated into methanol, filtered, and dried under vacuum to achieve the desired polymer (85 mg). The purified material was over 90% regioregular by NMR and had a molecular weight by GPC of M_w 16 000; M_n 10 000 g/mol.

For all spectroscopic measurements on pure P3TV solutions, the polymer was dissolved in toluene to a concentration of 250 μg/mL unless otherwise noted. Measurements using chlorobenzene or *ortho*-dichlorobenzene solutions yielded identical results. Triplet reference spectra were obtained through triplet sensitization as per Apperloo et al.[30] For these measurements, P3TV and *N*-methylfulleropyrrolidine were dissolved together in *ortho*-dichlorobenzene in a nitrogen-filled glovebox to final concentrations of 200:240 μg/mL, respectively. To test for quenching of triplets by oxygen, the mixed P3TV:NMFP solutions were bubbled with air for 1 min. In all measurements, samples were kept in sealed quartz cuvettes (Hellma Analytics) with 1 mm path length.

Subpicosecond transient absorption (TA) measurements were performed on a previously reported setup[8] with slight modifications. Narrow-band (~10 nm) excitation pulses were generated in an optical parametric amplifier (TOPAS, Light Conversion Ltd.) coupled to the output of a 1 kHz regenerative amplifier (Spectra-Physics Solstice), affording a time resolution of approximately 120 fs. Pump photon energies ranged from 1.9 to 2.6 eV, with typical pump fluences below 2×10^{14} photons/pulse cm^2. Because excessive pump fluence results in spurious ultrafast effects, all measurements were also performed at lower fluence, and the fluence dependence was studied in detail for three pump photon energies (Figure S1, Supporting Information). No dependence was found in the range used. The sample transmission was probed using broadband pulses generated in two home-built noncollinear optical parametric amplifiers (NOPAs) roughly spanning 0.75−2.5 eV.[31,32] The probe beam was split to provide a reference signal not affected by the pump to mitigate any laser fluctuation effects, and both were dispersed in a spectrometer (Andor, Shamrock SR-303i) and detected using a pair of linear image sensors (Hamamatsu, G11608) driven and read out at the full laser repetition rate by a custom-built board from Stresing Entwicklungsbüro. The differential transmission ($\Delta T/T$) was then measured as a function of probe photon energy and temporal pump−probe delay. The same setup was employed for nanosecond TA, using the frequency-doubled (2.33 eV) or -tripled (3.50 eV) nanosecond output of a Q-switched Nd:YVO_4 laser as the excitation source. High-time-resolution measurements were also performed on a similar setup, in which both the pump and probe beams were generated by homemade NOPAs generating sub-20-fs (pump) and sub-10-fs (probe) pulses using chirped mirror compression.

■ RESULTS

Figure 1 shows the absorption spectrum of P3TV in solution (solid), which is broadly consistent with previous reports.[22,25,33−35] We note, however, that the band edge and 0−0/0−1 peak ratio vary quite strongly with the synthetic route chosen. The band edge we observe here at ~1.85 eV suggests a mean conjugation length of 10−12 thienylenevinylene units from comparison with oligomer results.[30] This is 100 meV higher than the band gap reported by Olejnik et al.,[25] which we attribute to the different regioregularity and conjugation length in that work. The spectral shape was found to be invariant over 4 orders of magnitude of concentration (0.4 μg to 4.0 mg/mL; see Figure S2), and we specifically highlight the absence over the entire concentration range of the well-characterized low-energy shoulder assigned to aggregated chains.[22,25,33] We can thus confirm that the samples used for spectroscopy correspond to the isolated chain limit, and the solution photophysics described below can be attributed entirely to

dx.doi.org/10.1021/ja405427j | J. Am. Chem. Soc. 2013, 135, 12747−12754

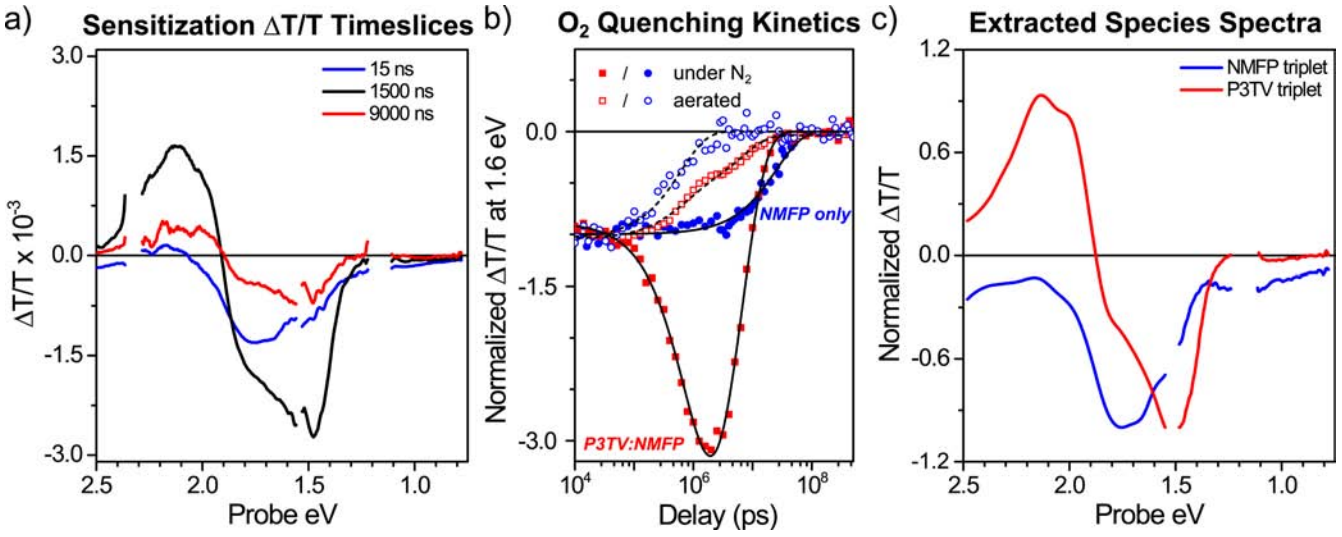

Figure 2. Triplet sensitization in P3TV. (a) TA timeslices of P3TV:NMFP mixed solution excited at 2.33 eV by nanosecond pulses. (b) Kinetics of the PIA signal at 1.6 eV (symbols), normalized to the value at 10 ns and fitted with exponential decays (black). Circles are NMFP only, squares are P3TV:NMFP mixed solutions. Lifetimes determined by fits to the data in N_2/air: P3TV, 6.0 μs/6.5 μs; NMFP, 25.6 μs/625 ns. (c) Normalized species-associated $\Delta T/T$ spectra extracted from the data in (a).

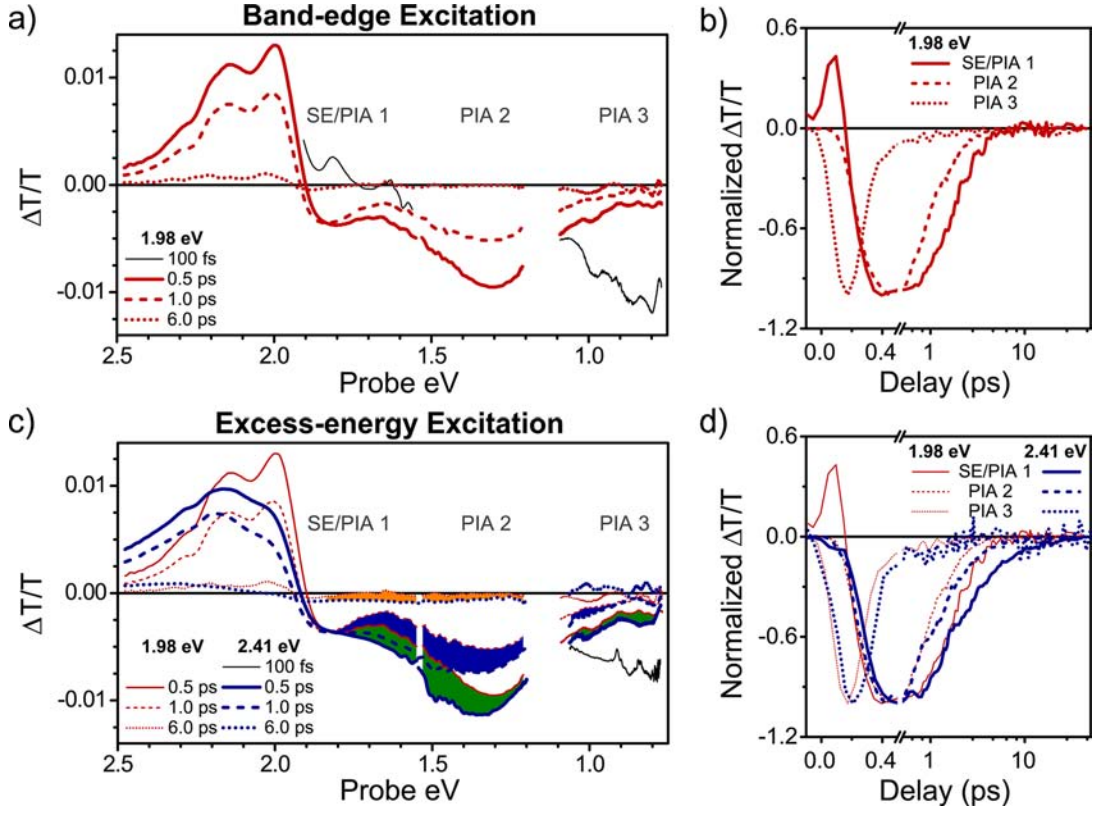

Figure 3. Band-edge versus excess-energy excitation. (a) TA spectra of P3TV in solution at selected timeslices for excitation near the band edge. Black trace shows stimulated emission and $1B_u$ PIA detected within the instrument response upon band-edge excitation. Other spectral regions were removed for clarity. (b) Decay kinetics of band-edge TA taken at 1.77 eV (SE/PIA1), 1.31 eV (PIA2), and 0.83 eV (PIA3). (c) TA spectra from the same sample obtained from midband excitation (blue) compared with band-edge data (red). The filled regions indicate the additional PIA arising from excess energy excitation. (d) Decay kinetics of midband TA taken at the same probe energies as in (b).

intrachain processes. Upon film formation (dotted), the main absorption band scarcely shifts but we do observe the formation of the aggregate shoulder.

P3TV Triplet Sensitization. As this study is concerned with triplet excitons on P3TV, we first establish the spectral signature and lifetime of P3TV triplets using the sensitization procedure reported by Apperloo et al.[30] Representative transient absorption (TA) timeslices are presented in Figure 2a. Our TA results are presented throughout in units of $\Delta T/T$, in which the absorption of photogenerated states appears negative. Positive features can reflect either increased transmission of the probe through the sample due to bleaching of

dx.doi.org/10.1021/ja405427j | J. Am. Chem. Soc. 2013, 135, 12747−12754

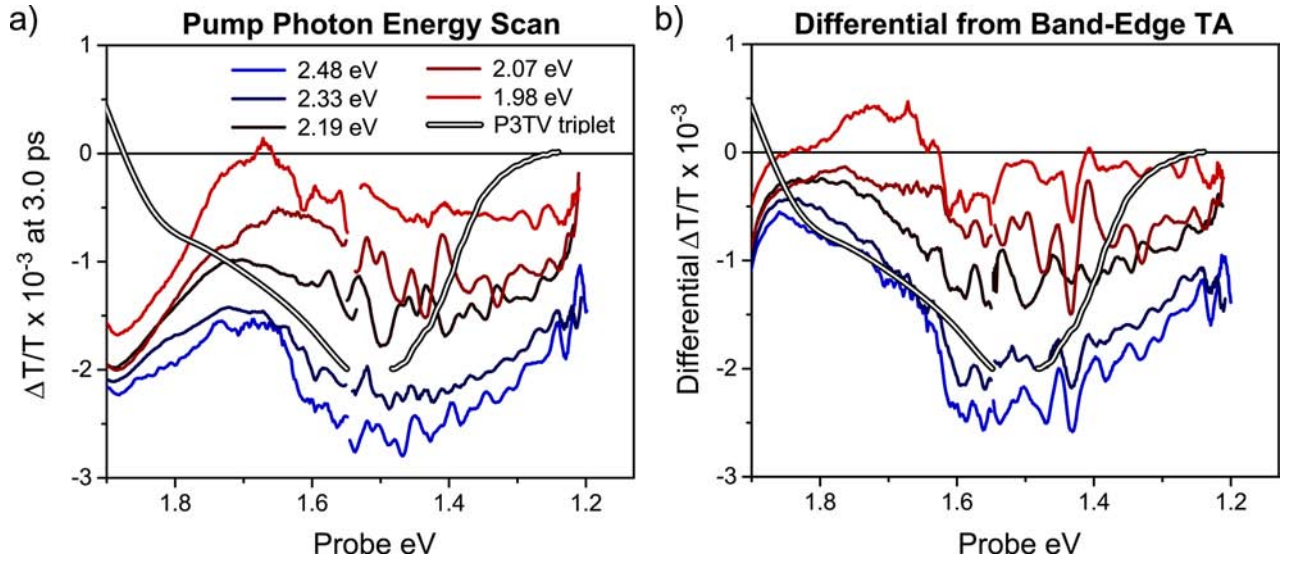

Figure 4. TA pump series. (a) TA timeslices of P3TV at 3.0 ps, showing increased triplet yield with increasing pump photon energy. The full spectral range and complete pump series are presented in Figure S5c. The P3TV triplet spectrum is taken from Figure 2c. (b) TA timeslices after subtraction of band-edge excitation data, showing close agreement with triplet PIA.

the ground state or additional intensity arising from stimulated emission. A mixed solution of P3TV and *N*-methylfulleropyrrolidine (NMFP, absorption spectrum in Figure S3a) was excited using nanosecond pulses at 2.33 eV, producing a large population of P3TV and NMFP singlets. Direct excitations of P3TV are extremely short-lived (see below) and the fullerene undergoes rapid intersystem crossing, resulting in a large population of triplet excitons predominantly on NMFP shortly after the instrument response (blue trace). Diffusional collisions allow triplet energy transfer to the polymer and yield P3TV triplets, a mechanism that overwhelming favors the generation of at most one triplet per chromophore. This transfer can be clearly resolved on the μs time scale (black trace) due to the dramatically higher absorption cross-section of the polymer. The P3TV triplet excitons then decay with a lifetime of 6 μs (Figure 2b, red squares).

To confirm that direct excitation of P3TV does not interfere with this mechanism, we repeated the measurement using selective excitation of the fullerene at 3.50 eV and obtained identical results at delays beyond the P3TV singlet lifetime (Figure S3b). We note that charge transfer from NMFP to P3TV is also a viable decay pathway, but can rule this out here due to the absence in the spectra of the broad photoinduced absorption (PIA) in the IR typically associated with polymer polarons.[24] As shown in Figure 2c, the TA data for this system can be decomposed using singular value decomposition into triplet excitons on NMFP, with a broad visible PIA, and on P3TV, characterized by a strong PIA at 1.55 eV crossing over at 1.88 eV to ground-state bleach (GSB). The P3TV triplet PIA agrees well with the band observed by Apperloo et al. in sensitized long oligomers in solution.[30] However, Lafalce et al.[24] measure a triplet absorption at significantly lower energies in P3TV films using quasi-steady-state PIA. We attribute this discrepancy to interchain effects in the solid state and the markedly longer time scales accessed by PIA. This technique preferentially detects isolated, deeply trapped triplets.

While it can be difficult to precisely determine triplet energy levels in the absence of phosphorescence, an energy threshold can be established through oxygen exposure. Oxygen is known to efficiently quench triplets whose energy is above 1 eV through the production of singlet oxygen.[36] In pure NMFP solutions, we see this effect as a drop in the fullerene triplet decay lifetime from 26 μs under N_2 to 625 ns after aeration (circles in Figure 2b). In the mixed solutions, this quenching is competitive with diffusional triplet energy transfer (time constant ~1 μs) and is reflected in the sharply reduced yield of P3TV triplets. However, the polymer triplet excitons that are generated exhibit the same lifetime, 6 μs, independent of the presence of O_2, as shown by the fits in Figure 2b. Thus, we conclude the P3TV triplet energy lies below 1 eV.

P3TV Band-Edge Excitation. To resolve the photophysics of P3TV upon direct photoexcitation, we turn to subpicosecond TA and begin with a pump photon energy just above the band edge. As shown in Figure 3a (black lines), under excitation at 1.98 eV, we observe three features within the instrument response: a pronounced GSB at 1.9−2.5 eV, a set of positive peaks just to the red of the band edge at 1.6−1.8 eV, and a PIA below 1.0 eV (PIA3). The positions of the positive peaks closely match the photoluminescence spectrum reported for P3TV solutions by Olejnik et al.[25] (Figure S4), enabling us to assign them to stimulated emission (SE) from the initial $1B_u$ exciton. We note that the SE band is overlapped with absorption bands PIA1 and PIA2 and may also overlap with PIA from the $1B_u$ exciton. Thus, even within the pulse duration part of the SE appears as a negative signal, and it is rapidly pulled beneath $\Delta T/T = 0$ while its peaked structure can still be distinguished. The SE and PIA3 both decay with the same instrument-limited kinetics (Figure 3b) and thus arise from the same excited state, which puts an upper limit on the $1B_u$ lifetime of ~130 fs. The $1B_u$ decay is matched by the simultaneous rise of the PIA2 band extending from 0.9 to 1.7 eV, which is the dominant spectral feature by 0.5 ps. This band is assigned to a transition from the $2A_g$ state, and its rapid formation reflects the well-known ultrafast internal conversion from $1B_u$ to $2A_g$.[24,25,30,37] The $2A_g$ state (PIA2) decays, with a 0.9 ps time-constant, to the ground state ($1A_g$) via efficient internal conversion. Such rapid nonradiative decay is typical in polyenes due to strong coupling to the vibrational manifold and

dx.doi.org/10.1021/ja405427j | J. Am. Chem. Soc. 2013, 135, 12747−12754

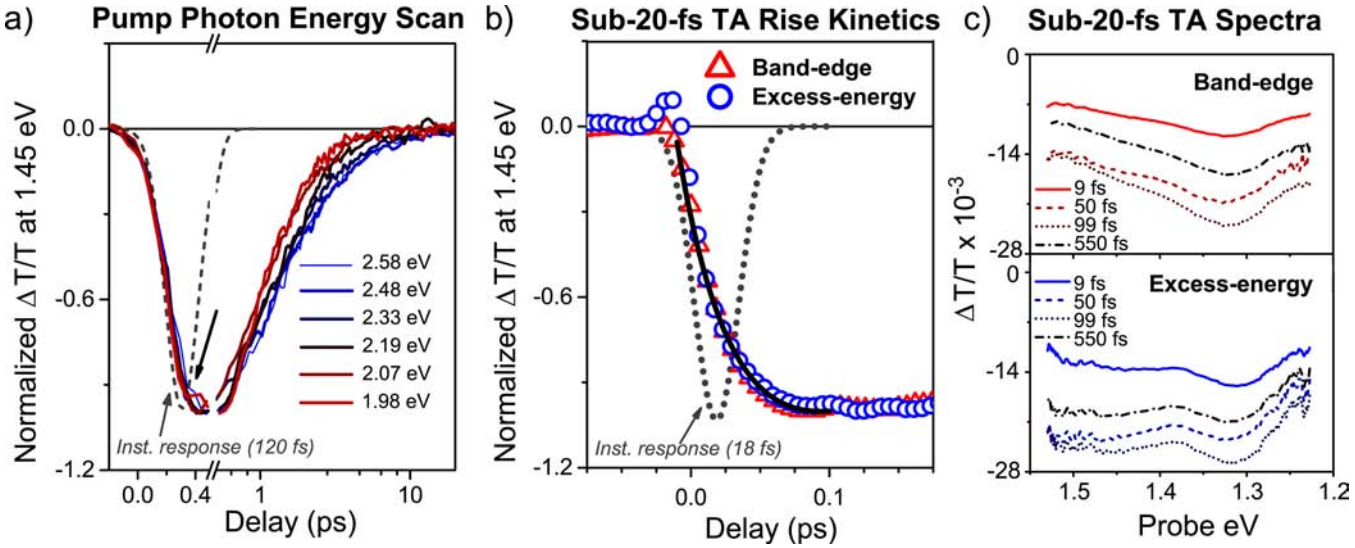

Figure 5. Parallel triplet and $2A_g$ formation. (a) Integrated kinetics at 1.45 eV for the pump series in Figure 4. Excess energy slows the final decay but does not affect the rise. Black arrow indicates the region where slightly slower rise can be distinguished for 2.58 eV excitation. (b) Rise kinetics of the triplet and $2A_g$ PIA at 1.45 eV using sub-20-fs TA. Black line is an exponential fit with 45 fs rise constant. (c) TA timeslices from the sub-20-fs measurement.

to the similarity of the excited ($2A_g$) and ground ($1A_g$) states.[38] It has been shown in the solid state that this fast decay releases significant vibrational energy.[25] Likewise, in solution, this effect produces a vibrationally excited ground state with a slightly red-shifted absorption band. This process is reflected in the increasing relative prominence of the distinctive PIA at 1.85 eV (PIA1), which decays on a picosecond time scale. We see, then, that band-edge excitation results in the purely singlet dynamics that are described in the conventional model of P3TV in Figure 1b.

P3TV Mid-Band Excitation. The same essential features, PIA1, PIA2, and PIA3, are reproduced under midband excitation at 2.41 eV (Figure 3c, blue). In particular, we note that PIA3, the signature of $1B_u$, is independent of excitation energy. This indicates both excitation conditions result in the same initial exciton with the same mean conjugation length. The primary spectral difference observed when exciting with excess energy is the appearance of an additional PIA from 1.2 to 1.8 eV (shaded areas in Figure 3c). This additional absorption was reproduced in Figures 4a and S5 over a range of 10 pump photon energies from 1.9 to 2.6 eV. We observed a progressive increase in its prominence with increasing pump photon energy beyond a threshold of ~2.1 eV (circles, Figure 1a), indicating optical activation of an alternative decay channel. As a guide to the eye for identifying this new band, in Figure 4b, we have directly subtracted the band-edge TA spectra (1.9 eV pump) from all other spectra, after scaling to account for excitation density. Such scaling is justified here, as we are operating well within the linear response regime across the entire excitation energy scan (Figure S1). Comparison of these differential spectra with the P3TV triplet PIA identified above shows that the new band closely matches the triplet absorption, particularly around the absorption maximum. There is a clear broadening of the band on the low-energy side, which has been attributed in a similar system to interaction between a correlated pair of triplet excitons confined to a one-dimensional polymer chain.[18,19] It is also possible for excitation with excess energy to result in fast polaron pair generation. Reported P3TV and oligomer polaron spectra[24,30] show pronounced absorption in the range 0.8−1.2 eV and no strong peaks at 1.5 eV. This absorption profile does not match the additional absorption detected upon midband excitation; thus, we attribute the new feature to triplets. The triplet PIA is already strongly pronounced by the end of the instrument response, as seen in Figures 3c and S6, suggesting its formation rate is comparable to the $1B_u \rightarrow 2A_g$ internal conversion, that is, much faster than can be explained by spin−orbit coupling in such a low-atomic-mass system. Because of this fast triplet formation and the excitation energy dependence, we identify this pathway instead as singlet fission from a vibrationally excited state, that is, optically activated singlet fission. We note that the energy threshold of 2.1 eV is indeed more than sufficient energy for a pair of triplets, taken to be <2 eV on the basis of sensitization.

The question remains which state, "hot" $1B_u$ or $2A_g$, is the precursor for triplet formation, which we probe in greater detail through a careful study of the excitation energy dependence. The increase in triplet yield corresponds to a slight increase in lifetime (Figures 5a, S6), but the early time dynamics scarcely change. In particular, the signatures of $1B_u$ decay, namely, the decay of PIA3 and rise of PIA2 (Figures 3d and S6), are clearly independent of pump photon energy up to 2.48 eV. We observe none of the standard signs of vibrational relaxation in the $1B_u$ manifold. This fact is significant, as it requires that singlet fission and internal conversion from $1B_u$ occur on a faster time scale than vibrational relaxation. Indeed, within the instrumental resolution of these measurements the triplet and $2A_g$ states appear to be formed in parallel. Thus, we tentatively assign the $1B_u$ state as the precursor for singlet fission, an assignment confirmed below using high-time-resolution TA. Interestingly, in all cases the triplet decay lifetime is extremely short (<10 ps). We propose this surprising behavior is due to confinement of the triplet pair on single polymer chains, allowing facile recombination to a singlet-character triplet-pair state and subsequent rapid decay to the lower-lying $2A_g$ state, discussed below.

This picture changes somewhat for still higher-energy excitation. At 2.58 eV, we resolve a slower rise in most PIA

dx.doi.org/10.1021/ja405427j | J. Am. Chem. Soc. 2013, 135, 12747−12754

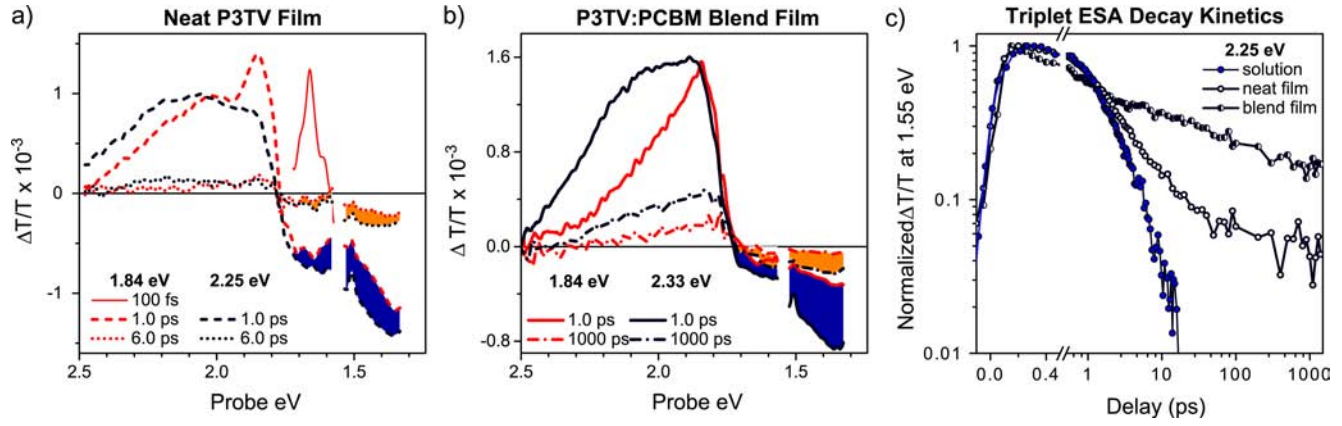

Figure 6. Singlet fission in the solid state. (a) TA timeslices for band-edge (red) and excess-energy (black) excitation showing enhanced triplet formation (filled regions) within neat P3TV films. (b) A still greater spectral enhancement is seen in blend films, with possible polaron formation by 1000 ps. (c) The lifetime of the PIA at 1.55 eV progressively increases from solution to neat film to blend.

features, as well as a distinctly slower decay of the initial $1B_u$ PIA (Figures 5a and S6). The GSB rise remains the same as for lower-energy excitation, though, meaning the difference is not simply due to reduced time resolution at this pump photon energy. Instead we propose excitation of a different excited state, for instance the nB_u level at 2.5 eV identified by Olejnik et al.[25] At 2.58 eV, there is thus enough energy to generate highly vibrationally excited $1B_u$ excitons but also "band-edge" nB_u excitons. These higher states appear to decay to $1B_u$ through internal conversion and then follow the same decay channels already outlined, with a net effect of slightly slowing the entire pathway. This is consistent with the results of Olejnik et al., in which the pump photon energy of 3.1 eV results in a direct excitation of nB_u and yields a still slower internal conversion time constant of 240 fs.[25] While the spectra acquired from upper-band excitation are broadly consistent with the picture presented above, the kinetics are greatly complicated by the introduction of this additional state. We thus restrict ourselves to noting that the discrepancies between the data in this work and ref 25 can be largely explained by the different character of the initial excited state, the different character (band edge and regioregularity) of the material, and our characterization of excitation energy dependence.

High Time Resolution TA. Because the $1B_u \rightarrow 2A_g$ internal conversion and singlet fission occur on time scales well below the 130 fs resolution attainable with the narrow-band excitation scheme, we also studied the effect of excess energy excitation with the sub-20-fs TA setup (Figures 5b and c, S7). The pump here is a temporally compressed broadband pulse, which for comparison was centered at either 2.38 eV ("excess-energy") or 2.07 eV ("band-edge"). Although this scheme results in much broader distributions of vibrationally excited $1B_u$ excitons, the same qualitative features of excess-energy excitation can be seen as in the narrow-band case: reduced SE, additional triplet PIA from 1.2 to 1.8 eV (Figure 5c) and longer decay lifetime. Monitoring the TA signal at 1.45 eV, which contains PIA contributions from the triplet and from $2A_g$, we see in Figure 5b that the rise kinetics is identical for band-edge and excess-energy excitation, that is, with and without triplet formation. At the same time, upon excess-energy excitation we can observe the pronounced triplet PIA even in the earliest timeslices of Figure 5c. These observations are not consistent with sequential formation of hot $2A_g$ and then triplets, and indeed the position of the $2A_g$ PIA is unaffected by excess energy excitation. Instead, the rise kinetics clearly show that given sufficient excess energy in the initial $1B_u$ exciton, singlet fission and internal conversion to $2A_g$ are parallel decay pathways from $1B_u$ with similar rates, possibly a consequence of the A_g symmetry of coupled triplet pairs in polyenes.[20] The time constants for these processes are both of the order of 45 fs, which is the fastest singlet fission rate observed for any organic system. It is likely that one of the key factors in such rapid singlet fission is its intramolecular nature; no intermolecular motion[39] should be required to accomplish fission.

Singlet Fission in Films. While solution-based measurements are of great utility in unravelling the mechanism of singlet fission in P3TV, the practically relevant question is whether fission persists in the solid state. As shown in Figure 6, the same process described in solution (fast appearance of the triplet PIA band at 1.55 eV under excess-energy excitation) is observed in spin-cast films. In the neat films, the triplet PIA is significantly longer lived than in solution. We note that the well-known P3TV thermal artifact[24,25] has no PIA component in this spectral region and is thus unlikely to give rise to these long-lived signatures (Figure S8b). Blending with PC60BM further increases the lifetime and results in a flatter PIA at long times, consistent with polaron formation on the polymer (Figure 6b).[40] This long-lived PIA exhibits an excitation energy dependence similar to the triplet, which suggests that singlet fission may contribute to charge formation. This is the first observation of charge formation following singlet fission in a bulk heterojunction structure. However, it does not appear to make a significant contribution to device performance, as solar cells using P3TV typically have low efficiencies (<1%).[35] We attribute this both to the fast nonradiative decay observed in solution and neat films and to fast charge recombination (Figure 6c, first 2 ps), possibly due to low mobility. The origin and fate of these charged species is the subject of a separate detailed study.

■ DISCUSSION

We have for the first time demonstrated optically activated singlet fission in P3TV. This process occurs under excess-energy excitation in isolated chains in solution as well as neat films and appears to contribute to polaron formation in blends with PC60BM. Our mechanism for intramolecular triplet generation in this material has precedent in previous studies of polydiactylene[17−19] and long polyenes.[20] However, the relation-

dx.doi.org/10.1021/ja405427j | J. Am. Chem. Soc. 2013, 135, 12747−12754

ship to observations of activated singlet fission in acene-based materials[41] is less clear: activated intermolecular singlet fission has only been conclusively observed through excitation into higher-lying singlet states, whereas in this work we excite into the same $1B_u$ manifold throughout. This important distinction is in line with the current view that singlet fission in polyenes proceeds through a different mechanism from that of the acenes.

We see that singlet fission in P3TV proceeds on a 45 fs time scale in parallel with the conventional nonradiative decay pathway through $2A_g$. This significant finding demands a re-evaluation of the standard mechanism of singlet fission in polyenes. We note that the theory of fission in materials with a low-lying A_g state is grounded in the symmetry of this state. It is generally considered to have significant doubly excited character and resemble a pair of triplets weakly coupled into an overall singlet.[21] The assumption has been that given an energetic push (i.e., excess energy) and sufficient space for the triplets to separate, such A_g states can readily undergo fission into a triplet pair. In P3TV, however, the triplets are generated without passing through the $2A_g$ state. The initial $1B_u$ exciton decays in all cases through ultrafast internal conversion to the A_g manifold. Under band-edge excitation, this yields only the $2A_g$ state, whereas excess-energy excitation enables the parallel formation of a higher-lying state of A_g symmetry, the triplet pair. The triplets are thus formed directly in the internal conversion from $1B_u$ into the A_g manifold. Our model is consistent with suggestions from work on other polyenes, in which no sign of a precursor $2A_g$ state could be detected.[20,27] This work, though, is the first with sufficient time resolution under excess-energy excitation to directly observe the simultaneous formation of triplets and the lower-lying $2A_g$ state.

The primary role of the $2A_g$ state is in the fast triplet decay. In solution, the triplets produced through fission remain confined to the same polymer chain and weakly coupled to the singlet manifold. Because the $2A_g$ state has a lower energy than the triplet pair and the same symmetry, fast relaxation into it after singlet fission is expected. This then enables the same efficient nonradiative decay pathway from $2A_g$ back to the ground state seen under band-edge excitation. Hence, the triplet pair lifetime after intrachain fission is shorter than 10 ps, compared to an isolated triplet lifetime of 6 μs observed in the sensitization experiment. In the solid state, triplet diffusion to traps can break the spin symmetry required to couple the triplet pair into the singlet manifold, making $2A_g$ no longer an effective decay pathway. This leads to significantly enhanced lifetimes. In blend films with a suitable electron acceptor such as PC60BM, the lifetime is still further enhanced by charge transfer from the triplet state.

CONCLUSIONS

Our results suggest a new design principle for ultrafast singlet fission sensitizers which may largely avoid the strong geometric dependence typical of planar materials: highly extended π systems with sufficient space to accommodate two distinct triplet excitons.

On a more fundamental level, polyenes like P3TV offer a potent experimental platform to investigate the mechanism of singlet fission. We see that singlet fission in P3TV is effectively the intramolecular analogue of the well-studied intermolecular fission processes in the acenes, which is endothermic for anthracene,[1] energy neutral or slightly endothermic for tetracene[12] and exothermic for pentacene.[8−11] Because of the ultrafast relaxation from $2A_g$ back to the ground state, fission in P3TV cannot be induced through thermal activation alone. However, given sufficient energy in the initial excitation to make fission exothermic (i.e., above the 2.1 eV threshold), the system resembles pentacene: triplets are formed on time scales even faster than vibrational relaxation. It remains an open question whether and how the mechanism of such ultrafast triplet generation differs between the intermolecular pentacene and intramolecular polyene regimes. One of the primary advantages of this intramolecular system is that the relevant energy levels can be readily tuned through chemical modification. This should enable control over the interplay between activated and exothermic regimes, providing valuable insight into the mechanism of singlet fission.

ASSOCIATED CONTENT

Supporting Information

NMR spectra, concentration and pump fluence dependence, comprehensive TA data, and thermal effects. This material is available free of charge via the Internet at http://pubs.acs.org.

AUTHOR INFORMATION

Corresponding Author

am956@cam.ac.uk

Notes

The authors declare no competing financial interest.

ACKNOWLEDGMENTS

This work was supported by the EPSRC (UK) (EP/G060738/1), the European Community (FP-7 INFRASTRUCTURES-2008-1, 'Laserlab Europe II', Contract No. 228334; and Marie-Curie ITN-SUPERIOR, PITN-GA-2009-238177), the Royal Society Dorothy Hodgkin Fellowship, and the Winton Programme for the Physics of Sustainability.

REFERENCES

(1) Smith, M. B.; Michl, J. *Chem. Rev.* **2010**, *110*, 6891.
(2) Hanna, M. C.; Nozik, A. J. *J. Appl. Phys.* **2006**, *100*, 074510.
(3) Jadhav, P. J.; Mohanty, A.; Sussman, J.; Lee, J.; Baldo, M. A. *Nano Lett.* **2011**, *11*, 1495.
(4) Ehrler, B.; Wilson, M. W. B.; Rao, A.; Friend, R. H.; Greenham, N. C. *Nano Lett.* **2012**, *12*, 1053.
(5) Ehrler, B.; Walker, B. J.; Böhm, M. L.; Wilson, M. W. B.; Vaynzof, Y.; Friend, R. H.; Greenham, N. C. *Nat. Commun.* **2012**, *3*, 1019.
(6) Ehrler, B.; Musselman, K. P.; Böhm, M. L.; Friend, R. H.; Greenham, N. C. *Appl. Phys. Lett.* **2012**, *101*, 153507.
(7) Jadhav, P. J.; Brown, P. R.; Thompson, N.; Wunsch, B.; Mohanty, A.; Yost, S. R.; Hontz, E.; Van Voorhis, T.; Bawendi, M. G.; Bulovic, V.; Baldo, M. A. *Adv. Mater.* **2012**, *24*, 6169.
(8) Rao, A.; Wilson, M. W. B.; Hodgkiss, J. M.; Albert-Seifried, S.; Bässler, H.; Friend, R. H. *J. Am. Chem. Soc.* **2010**, *132*, 12698.
(9) Wilson, M. W. B.; Rao, A.; Clark, J.; Kumar, R. S. S.; Brida, D.; Cerullo, G.; Friend, R. H. *J. Am. Chem. Soc.* **2011**, *133*, 11830.
(10) Rao, A.; Wilson, M. W. B.; Albert-Seifried, S.; Di Pietro, R.; Friend, R. H. *Phys. Rev. B* **2011**, *84*, 195411.
(11) Chan, W. L.; Ligges, M.; Jailaubekov, A.; Kaake, L.; Miaja-Avila, L.; Zhu, X.-Y. *Science* **2011**, *334*, 1541.
(12) Burdett, J. J.; Bardeen, C. J. *J. Am. Chem. Soc.* **2012**, *134*, 8597.
(13) Johnson, J. C.; Nozik, A. J.; Michl, J. *Acc. Chem. Res.* **2013**, *46*, 1290.
(14) Roberts, S. T.; McAnally, R. E.; Mastron, J. N.; Webber, D. H.; Whited, M. T.; Brutchey, R. L.; Thompson, M. E.; Bradforth, S. E. *J. Am. Chem. Soc.* **2012**, *134*, 6388.
(15) Ma, L.; Zhang, K.; Kloc, C.; Sun, H.; Michel-Beyerle, M. E.; Gurzadyan, G. G. *Phys. Chem. Chem. Phys.* **2012**, *14*, 8307.

(16) Yamagata, H.; Spano, F. C. *J. Chem. Phys.* **2012**, *136*, 184901.
(17) Kraabel, B.; Hulin, D.; Aslangul, C.; Lapersonne-Meyer, C.; Schott, M. *Chem. Phys.* **1998**, *227*, 83.
(18) Lanzani, G.; Stagira, S.; Cerullo, G.; De Silvestri, S.; Comoretto, D.; Moggio, I.; Cuniberti, C.; Musso, G. F.; Dellepiane, G. *Chem. Phys. Lett.* **1999**, *313*, 525.
(19) Lanzani, G.; Cerullo, G.; Zavelani-Rossi, M.; De Silvestri, S.; Comoretto, D.; Musso, G.; Dellepiane, G. *Phys. Rev. Lett.* **2001**, *87*, 187402.
(20) Antognazza, M. R.; Lüer, L.; Polli, D.; Christensen, R. L.; Schrock, R. R.; Lanzani, G.; Cerullo, G. *Chem. Phys.* **2010**, *373*, 115.
(21) Tavan, P.; Schulten, K. *Phys. Rev. B* **1987**, *36*, 4337.
(22) Zhang, C.; Matos, T.; Li, R.; Sun, S.-S.; Lewis, J. E.; Zhang, J.; Jiang, X. *Polym. Chem.* **2010**, *1*, 663.
(23) Xie, H.-Q.; Liu, C.-M.; Guo, J.-S. *Eur. Polym. J.* **1996**, *32*, 1131.
(24) Lafalce, E.; Jiang, X.; Zhang, C. *J. Phys. Chem. B* **2011**, *115*, 13139.
(25) Olejnik, E.; Pandit, B.; Basel, T.; Lafalce, E.; Sheng, C.-X.; Zhang, C.; Jiang, X.; Vardeny, Z. V. *Phys. Rev. B* **2012**, *85*, 235201.
(26) Lafalce, E.; Toglia, P.; Zhang, C.; Jiang, X. *Appl. Phys. Lett.* **2012**, *100*, 213306.
(27) Wang, C.; Tauber, M. L. *J. Am. Chem. Soc.* **2010**, *132*, 13988.
(28) Wang, C.; Schlamadinger, D. E.; Desai, V.; Tauber, M. J. *ChemPhysChem* **2011**, *12*, 2891.
(29) Al-Hashimi, M.; Baklar, M. A.; Colleaux, F.; Watkins, S. E.; Anthopoulos, T. D.; Stingelin, N.; Heeney, M. *Macromolecules* **2011**, *44*, 5194.
(30) Apperloo, J. J.; Martineau, C.; van Hal, P. A.; Roncali, J.; Janssen, R. A. J. *J. Phys. Chem. A* **2002**, *106*, 21.
(31) Manzoni, C.; Polli, D.; Cerullo, G. *Rev. Sci. Instrum.* **2006**, *77*, 023103.
(32) Cirmi, G.; Brida, D.; Manzoni, C.; Marangoni, M.; De Silvestri, S.; Cerullo, G. *Opt. Lett.* **2007**, *32*, 2396.
(33) Gavrilenko, A. V.; Matos, T. D.; Bonner, C. E.; Sun, S.-S.; Zhang, C.; Gavrilenko, V. I. *J. Phys. Chem. C* **2008**, *112*, 7908.
(34) Horie, M.; Shen, I.-W.; Tuadhar, S. M.; Leventis, H.; Haque, S. A.; Nelson, J.; Saunders, B. R.; Turner, M. L. *Polymer* **2010**, *51*, 1541.
(35) Zhang, C.; Sun, J.; Li, R.; Sun, S.-S.; Lafalce, E.; Jiang, X. *Macromolecules* **2011**, *44*, 6389.
(36) Schweitzer, C.; Schmidt, R. *Chem. Rev.* **2003**, *103*, 1685.
(37) Frolov, S.; Leng, J. M.; Vardeny, Z. V. *Mol. Cryst. Liq. Cryst.* **1994**, *256*, 473.
(38) Clark, J.; Tretiak, S.; Nelson, T.; Cirmi, G.; Lanzani, G. *Nat. Phys.* **2012**, *8*, 225.
(39) Zimmerman, P. M.; Zhang, Z.; Musgrave, C. B. *Nat. Chem.* **2010**, *2*, 648.
(40) Stevens, M.; Silva, C.; Russell, D. M.; Friend, R. H. *Phys. Rev. B* **2001**, *63*, 165213.
(41) Ma, L.; Galstyan, G.; Zhang, K.; Kloc, C.; Sun, H.; Soci, C.; Michel-Beyerle, M. E.; Gurzadyan, G. G. *J. Chem. Phys.* **2013**, *138*, 184508.